European Journal of Medicinal Chemistry 62 (2013) 738–744

Contents lists available at SciVerse ScienceDirect

European Journal of Medicinal Chemistry

journal homepage: http://www.elsevier.com/locate/ejmech

Original article

Synthesis and structure–activity relationships for 1-(4-(piperidin-1-ylsulfonyl) phenyl)pyrrolidin-2-ones as novel non-carboxylate inhibitors of the aldo-keto reductase enzyme AKR1C3

Daniel M. Heinrich [a], Jack U. Flanagan [a,b], Stephen M.F. Jamieson [a,b], Shevan Silva [a], Laurent J.M. Rigoreau [c], Elisabeth Trivier [c], Tony Raynham [c], Andrew P. Turnbull [d], William A. Denny [a,b,*]

[a] Auckland Cancer Society Research Centre, The University of Auckland, Private Bag 92019, Auckland 1142, New Zealand
[b] Maurice Wilkins Centre for Molecular Biodiscovery, The University of Auckland, Private Bag 92019, Auckland 1142, New Zealand
[c] Cancer Research Technology Ltd, Wolfson Institute for Biomedical Research, The Cruciform Building, Gower St., London, WC1E 6BT, UK
[d] Cancer Research Technology Ltd, Birkbeck College, University of London, London, UK

ARTICLE INFO

Article history:
Received 16 October 2012
Received in revised form
24 January 2013
Accepted 27 January 2013
Available online 9 February 2013

Keywords:
Aldo-keto reductase
Inhibitor
Crystal structure
Computer aided drug design

ABSTRACT

High expression of the aldo-keto reductase enzyme AKR1C3 in the human prostate and breast has implicated it in the development and progression of leukemias and of prostate and breast cancers. Inhibitors are thus of interest as potential drugs. Most inhibitors of AKR1C3 are carboxylic acids, whose transport into cells is likely dominated by carrier-mediated processes. We describe here a series of (piperidinosulfonamidophenyl)pyrrolidin-2-ones as potent (<100 nM) and isoform-selective non-carboxylate inhibitors of AKR1C3. Structure–activity relationships identified the sulfonamide was critical, and a crystal structure showed the 2-pyrrolidinone does not interact directly with residues in the oxyanion hole. Variations in the position, co-planarity or electronic nature of the pyrrolidinone ring severely diminished activity, as did altering the size or polarity of the piperidino ring. There was a broad correlation between the enzyme potencies of the compounds and their effectiveness at inhibiting AKR1C3 activity in cells.

1. Introduction

Enzymes belonging to the aldo-keto reductase (AKR) 1C subfamily are important modulators of both the steroid hormone and the leukotriene cascades. Of the AKR1C enzymes, the C3 isoform (also known as type 5 17-β-hydroxysteroid dehydrogenase) is of particular interest because of its high expression in the human prostate and breast, where it is responsible for producing (and over-producing) testosterone, 17-β-estradiol and 20-α-hydroxyprogesterone [1]. As such, AKR1C3 is implicated in the development and progression of leukemias and of prostate and breast cancers [2], and to a lesser extent leukemias through its prostaglandin F synthase activity [3]. This has made them interesting targets for the development of inhibitory small-molecule drugs that could be of potential use in controlling these diseases, and a number of such compounds have been reported [4,5].

Important issues in such drug development are obtaining selectivity between the four isoforms AKR1C1-4, which play different biological roles [6] and between these and the cyclo-oxygenase (COX) enzymes. The latter is highlighted by the fact that many inhibitors of the AKR1C subfamily are structurally related to the NSAID class of COX inhibitors, such as the anthranilates flufenamic [7] (**1**), meclofenamic [8] (**2**) and mefenamic [9] (**3**) acids (Table 1). We have determined the crystal structures for a range of NSAIDs bound in the AKR1C3 active site [10,11] that show, along with flufenamic acid [7], that the drug carboxylate group occupies the oxyanion hole, making H-bonds to the Y55 and H117 residues. We have also recently shown [4] that a series of (dihydroisoquinolyl)sulfonamidobenzoic acids (e.g., **4**) are potent and very selective inhibitors of AKR1C3 (Table 1), with the carboxylate binding similarly in the oxyanion hole of the enzyme.

The majority of known AKR1C inhibitors are carboxylic acids, whose transport into cells is likely dominated by carrier-mediated

Abbreviations: AKR, aldo-keto reductase; COX, cyclo-oxygenase; DCM, dichloromethane; DMSO, dimethyl sulfoxide; NADPH, nicotinamide adenine dinucleotide phosphate; NSAID, non-steroidal anti-inflammatory drugs; PDB, Protein Data Bank; ROCS, rapid overlay of chemical structures; TEA, triethylamine; TFA, trifluoroacetic acid.

* Corresponding author. Auckland Cancer Society Research Centre, The University of Auckland, Private Bag 92019, Auckland 1142, New Zealand. Tel.: +649 923 6144.
E-mail address: b.denny@auckland.ac.nz (W.A. Denny).

0223-5234/$ – see front matter © 2013 Elsevier Masson SAS. All rights reserved.
http://dx.doi.org/10.1016/j.ejmech.2013.01.047

Table 1
Potency and selectivity of carboxylate-based AKR1C inhibitors.

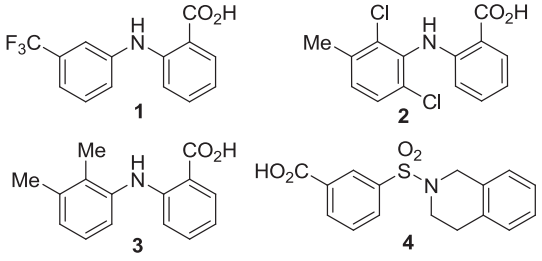

No	IC_{50} (μM)[a]					
	AKR1C1	AKR1C2	AKR1C3	AKR1C4	COX1[b]	COX2[b]
1	2.64	3.14	0.41	>100	3.0	9.3
2	3.16	8.74	0.54	>100	0.22	0.7
3	3.91	6.97	0.56	>100	25	2.9
4	20.3	>30	0.013	>30	>10	>10

[a] IC_{50} values are the average of 2 or more determinations.
[b] COX data for compounds **1**–**3** from Ref. [18]; for compound **4** from Ref. [4].

processes rather than passive diffusion [12], and thus difficult to predict. Therefore, we were interested that one of the hits from a high-throughput screen seeking novel and selective inhibitors of AKR1C3 was the pyrrolidine **12**, which was a very potent (IC_{50} 0.094 μM) and selective inhibitor [4]. Furthermore, in a cell-based assay evaluating analogues for their ability to block AKR1C3 from metabolising a known dinitrobenzamide substrate [4], **12** was more potent relative to its enzyme inhibitory activity than a carboxylic acid analogue (ratio IC_{50}(enz)/IC_{50}(cell) is 0.48 for **4** versus 8.5 for **12**), suggesting a pharmacological disadvantage for the acids in cells. We therefore undertook a study of the structure–activity relationships around the pyrrolidine lead **12**, and an investigation of its binding to the enzyme.

2. Chemistry

Compounds of Table 2, where the amide-containing ring was varied, were prepared from the halogenated sulfonamide intermediates **38a**–**k**, which were in turn prepared from known sulfonyl chlorides **36a**,**b** and substituted piperidines **37a**–**k** (Scheme 1). Reaction of **38a**–**k** with pyrrolidinone in the presence of CuI, *N*,*N*'-dimethylethylenediamine and K_2CO_3 gave compounds **10**, **12**–**21** in moderate yields. Compound **11** was prepared similarly from sulfonamide **39**. Compounds **22** and **23**, where the sulfonamide was replaced by amide and amine respectively, were prepared by coupling the benzoyl chloride **40** and benzyl bromide **41** with 2-methylpyrrolidine, and reacting the resultant intermediates **42**, **43** with 2-pyrrolidinone as above (Scheme 1).

The compounds of Table 3 fix the 2-methylpiperidine ring of **12** and vary the key pyrrolidone unit. Coupling of 2-methylpiperidine **37a** with substituted benzenesulfonic acids **36a**,**b**,**i**–**p** gave the corresponding sulfonamide intermediates **38a**,**b**,**i**–**p**, which were then reacted with 2-pyrrolidinine as before to give compounds **24**–**30** (Scheme 2). Reduction of the 4-nitro intermediate **38q** gave the amine **38r**, which was reacted with succinic or phthalic anhydride, pivaloyl or isobutyryl chloride or 3-chlorosulfonyl chloride to give respectively compounds **31**–**35** of Table 3.

3. Enzyme biochemistry and cell biology

The structures of the new compounds and their activities in the enzyme and cellular assays are shown in Tables 2 and 3. The

Table 2
Variation of the lipophilic binding moiety.

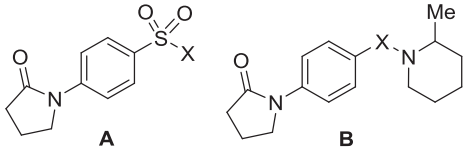

No	Fm	X	AKR (IC_{50}, μM)[a]			
			1C1	1C2	1C3	1C4
9	A	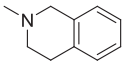	>30	>30	0.052	>30
10	A		>30	>30	0.14	>30
11	A				>30	
12	A		>30	>30	0.094	>30
13	A				11.88	
14	A		>30	>30	0.088	>30
15	A	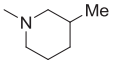	>30	>30	0.084	>30
16	A	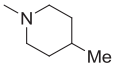	>30	>30	0.20	>30
17	A	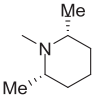	>30	>30	0.056	>30
18	A	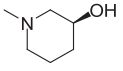	>30	>30	8.98	>30
19	A	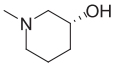	>30	>30	1.55	>30
20	A				>30	
21	A	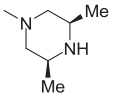			21.2	
22	B	C=O			>30	
23	B	CH_2			>30	

[a] IC_{50} values <10 μM are the mean for 2 or more determinations.

inhibitory activity of the compounds against the AKR1 isoforms C1–C4 was performed with a competitive fluorescence assay, where a non-fluorescent ketone probe (probe 5) [12] selective for the AKR1C enzyme isoforms is reduced to a fluorescent alcohol in the presence of AKR1C enzyme and NADPH. Compounds with biochemical IC_{50} values <100 nM were tested for activity at

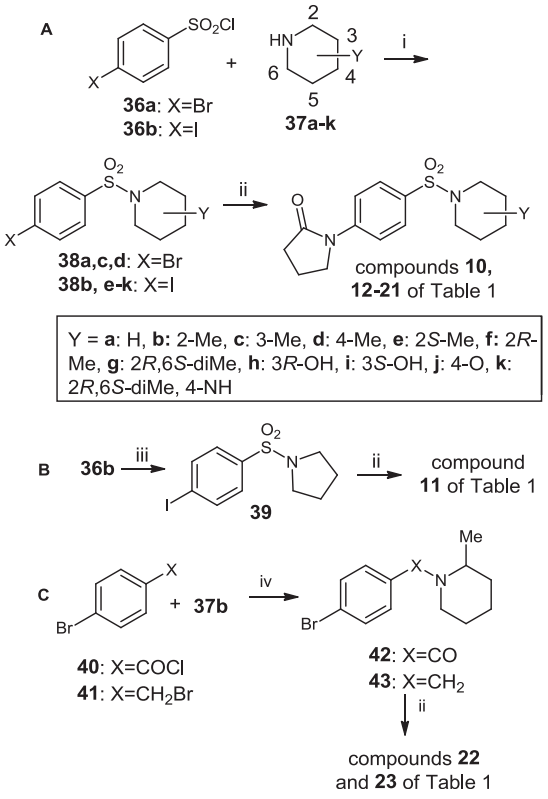

Scheme 1. Synthesis of the compounds of Table 1. Reagents and conditions: (i) DCM, TEA, piperidine, 20 °C; (ii) pyrrolidin-2-one, CuI, *N*,*N*'-dimethylethylenediamine, K_2CO_3, 100 °C, 18–24 h; (iii) pyrrolidine, TEA, DCM, 20 °C, 1 h; (iv) 2-methylpiperidine, TEA, DCM, 20 °C, 1 h (**40**)/K_2CO_3, tol, reflux, 3 h (**41**).

preventing the AKR1C3-dependent aerobic reduction of the dinitrobenzamide PR-104A to its hydroxylamine metabolite in an HCT116 cell line that overexpresses AKR1C3. Compound IC_{50} values were calculated by fitting the inhibition data to a four-parameter logistic sigmoidal dose–response curve using Prism 5.02 (GraphPad, La Jolla, CA, USA).

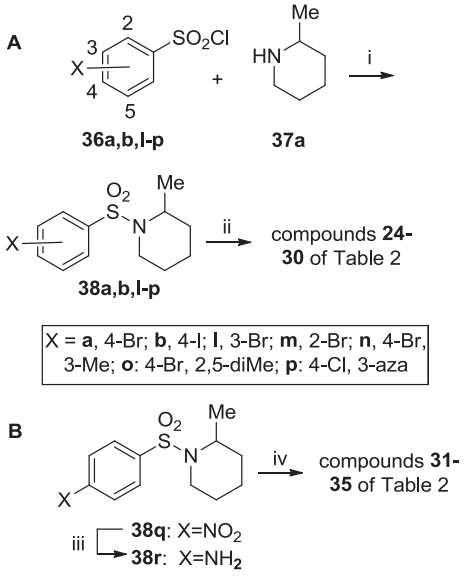

Scheme 2. Synthesis of the compounds of Table 2. Reagents and conditions: (i) DCM, TEA, piperidine, 20 °C; (ii) CuI, *N*,*N*'-dimethylethylenediamine, K_2CO_3, dioxane, 100 °C, 18–24 h; (iii) EtOAc, 10% Pd/C, H_2 (5 atm), 20 °C, 8 h; (iv) DCM, TEA, 20 °C.

Table 3
Variation of the pyrrolidinone binding unit.

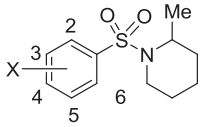

No	X	AKR (IC_{50}, μM)[a]			
		1C1	1C2	1C3	1C4
24	4- 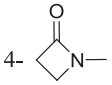	>30	>30	5.61	>30
25	4- 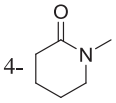	>30	>30	3.77	>30
26	3- 			>30	
27	2- 			>30	
28	4-  , 3-Me			10.2	
29	4-  , 2,5-diMe			>30	
30	4-  , 2-aza	>30	>30	2.77	>30
31	4- 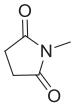			>30	
32	4- 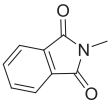			>30	
33	4-NHCOtBu	>30	>30	5.94	>30
34	4-NHCOiPr			12.5	
35	4- 	>30	>30	5.22	>30

[a] As for Table 2.

4. Crystallography

The structure of **12** bound in the AKR1C3 active site was determined by X-ray crystallography (PDB code 4H7C), as detailed previously [4]. This showed that unlike the carboxylate containing inhibitors with known binding modes, the pyrrolidinone unit made no direct contact to the oxyanion hole (Fig. 1), while the sulfonylpiperidine was located in the same pocket as the tetrahydroquinoline of **4** [4].

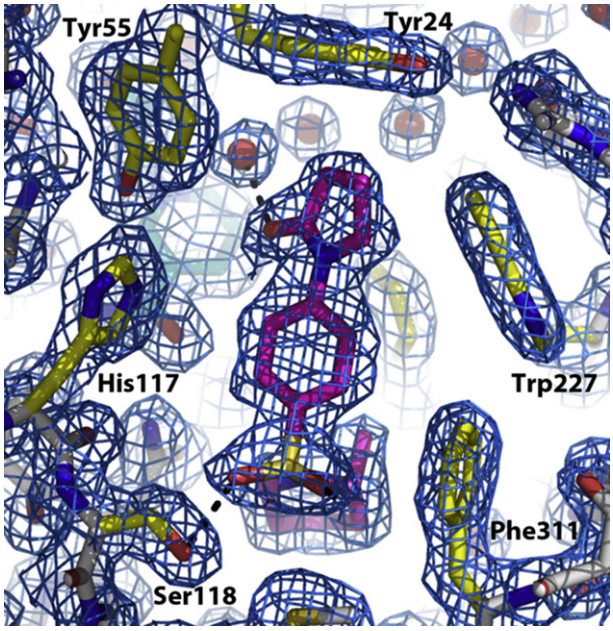

Fig. 1. Crystal structure of **12** complexed with AKR1C3. Protein Data Bank (PDB) code 4H7C. See Supplementary Material Table S1 for X-ray data collection and refinement information. Compound **12** is shown in magenta sticks, while. While key amino acids that define the pyrolidine-pheny-sulfone moiety binding site are labelled and shown in yellow sticks. Water molecules are represented as red spheres. Electron density of the ligand, NADP co-factor, water molecules and amino acids is also shown as a mesh. Interactions between the pyrrolindyl group and a water molecule, as well as the ligands sulponyl moiety and Ser118. (For interpretation of the references to colour in this figure legend, the reader is referred to the web version of this article.)

5. Results and discussion

The crystal structure of **12** bound in the AKR1C3 active site revealed that to accommodate the pyrrolidinone group at the 4 position of the phenylsulfone, compared to a carboxylate at the 3 position, the (methylsulfonyl)piperidine-phenyl was displaced further into the SP1 pocket [1] compared to **4** where it can interact with the side chain of Ser118. The compounds of Table 2 explore the role of the sulfonamide substituent and probe its fit to the enzyme hydrophobic pocket bounded by residues Met120, Asn167, Tyr216, Phe306, Phe311, Tyr317, Pro318 and Tyr319 (Fig. 1). In the acid series the dihydroisoquinoline appeared to be the preferred unit, as removal of the benzene ring caused a substantial (30-fold) loss of potency against AKR1C3 [3]. This is not the case in the 2-pyrrolidinone series, where there is only a 2.7-fold loss in potency going from the dihydroisoquinoline **9** to the piperidine **10**, and only 1.8 between **9** and the (racemic) 2-methylpiperidine **12**. This is of importance since the series is relatively insoluble compared to the previous acid series, and going from **9** to **10** markedly lowers the lipophilicity (Clog *P* from 3.35 to 2.49 respectively). However, there is a very marked dependence on ring size, with the pyrrolidine analogue **11** being completely inactive ($IC_{50} > 30$ μM). The dihydroisoquinoline unit of **9** may have an improved interaction with the SP1 pocket compared to the 2-methylpiperidine of **12** and contribute to the 1.8 fold increase in potency of **9** compared to **12**, although both compounds are 4 and 7 fold less potent than **4** respectively. This lower activity may result from the loss of an oxyanion hole interaction, along with the displacement of the butterfly shaped sulfonamide core common to the compounds. Exploration of the chirality of the methyl substituent on **11** showed that all the activity resides in the *R*-enantiomer **14** (IC_{50} 0.088 μM), which is 135-fold more potent than the corresponding *S*-enantiomer **13**, this is consistent with the *R*-enantiomer determined in the crystal structure. Compounds **15** and **16** probe the positioning of the methyl group; the 3-methyl analogue **15** is as potent as **12**, but the 4-methyl analogue **16** loses some potency.

With the crystal structure in hand, we next sought to identify sites for incorporating additional methyl and hydroxyl units around the 2*R*-piperidine ring. A series of analogues that investigated these substitutions at the 5- and 6-positions were modelled into the active site by superimposition onto **12** using ROCS (Rapid Overlay of Chemical Structures, Openeye Scientific Software), and energy minimised within the active site (the structures considered are illustrated in Table S2). Substitution patterns within the methyl or hydroxyl series with the lowest ligand-protein energy guided further analogue synthesis. Data for the analogues synthesised is presented in Table 2. The 2*S*,6*S*-dimethyl analogue **17** is as potent as the lead **12**, and has the lowest interaction energy within the dimethyl substituted series. The activity data for compounds **18** and **19** indicate that a hydroxyl group in this region of the active site is not favoured, although there is an enantiomeric preference, with stereoisomer **19** preferred over **18**. This preference is consistent with the energy values calculated for similar compounds with equivalent hydroxyl substitutions (Table S2).

Compounds **20**–**21** explore polarity in the ring, which is clearly deleterious, with the morpholine **20** and piperazine **21** losing all activity. Finally, the role of the sulfonamide linker was examined with the corresponding amide and amine **22** and **23**. As expected, these compounds were completely inactive, consistent with the sulfonyl providing a rigid directionality in the molecule that pre-arranges it for the AKR1C3 active site.

The compounds of Table 3 examine the role of the 2-pyrrolidinone. The crystal structure of **12** bound to the enzyme (Fig. 1) shows that while this does not make direct H-bond contacts with the Y55 and H117 residues that constitute the "oxyanion hole" as does the carboxylate of **4**, the pyrrolidinone does occupy the SP3 pocket. The nature and positioning of the pyrrolidinone is therefore expected to be important, and this was confirmed. The ring size of the cyclic amide is critical, with the azetidinone **24** and piperidone **25** having IC_{50}s for AKR1C3 respectively 60-fold and 40-fold less than that of **12**. Moving the pyrrolidinone from the 4-position to either the 3-position (**26**) or the 2-position (**27**) lead to complete loss of activity (IC_{50}s > 30 μM). Keeping the pyrrolidinone at the 4-position but altering its conformation by steric crowding from a flanking 2-methyl group on the central benzene ring (compound **28**) diminished activity very severely. The corresponding 2,5-dimethyl analogue **29**, where the sulfonamide conformation may also be affected, was completely inactive. Interestingly, while altering the electronics of the central ring by making it a pyridine (**30**) also reduced activity, it was less severe. However, altering the electronics (rather than the conformation or position) of the pyrrolidine abolishes activity (pyrrolidine-2,5-dione **31**, indoline-1,3-dione **32**). Linear amides **33** and **34** retain some, but greatly diminished, activity, as does the isothiazolidine dioxide **35**. Overall, this SAR supports the crystal structure, suggesting that positioning of the pyrrolidine oxygen is constrained by the SP3 pocket and required for the compound to make the necessary H-bond to the structured water molecule.

The selectivity for AKR1C3 over other human AKR1C isoforms was determined for all compounds with IC_{50} values <10 μM, but none were active at inhibiting AKR1C1, 2 or 4 (IC_{50} values > 30 μM) (Tables 2 and 3). Representative compounds **10** and **12** were also evaluated for inhibition of the cyclooxygenase enzymes COX-1 and COX-2, and were found to be inactive at 10 μM.

All compounds with AKR1C3 IC_{50} values <100 nM were evaluated for their ability to block enzyme activity in human HCT-116 colon cancer cells engineered to over-express AKR1C3. Inhibitory activity was assessed by measuring the inhibition of AKR1C3

catalysed metabolism of an exogenous dinitrobenzamide substrate, PR-104A, exclusively metabolised by AKR1C3 under aerobic conditions to its cytotoxic hydroxylamine (PR-104H) and amine (PR-104M) metabolites [14]. As shown previously for a series of carboxylate-based inhibitors (e.g., **4**) [4], the effectiveness of compounds at inhibiting AKR1C3 activity in these cells broadly correlated with their enzymic activity, but in the present case the compounds were 2–8 fold more potent in the cellular assay (Table 4). This contrasted with results for the carboxylate-based series [3], which were almost universally less potent in the cell-based assay. We speculate that this may be due to poorer passive uptake of the carboxylate series.

6. Conclusions

SAR studies of potent and selective non-carboxylate AKR1C3 inhibitor **12** showed that while the sulfonamide was still critical (cf **12** with **31**,**32**), as in the carboxylate series represented by **4** [4], there was much more tolerance for the sulfonamide substituent, with a range of monocyclic six-membered ring analogues retaining activity and AKR1C selectivity (Table 2). Crystal structure studies show that the 2-pyrrolidinone was located in the SP3 pocket but did not bind to the oxy-anion hole, and variations in the position, co-planarity or electronic nature of the pyrrolidinone ring abolished or severely diminished activity. The effectiveness of compounds at inhibiting AKR1C3 activity in cells broadly correlated with their enzyme inhibitory activity (Table 4).

7. Experimental protocols

7.1. General conditions

Final products were analysed by reverse-phase HPLC (Alltima C18 5 μm column, 150 × 3.2 mm; Alltech Associated, Inc., Deerfield, IL) using an Agilent HP1100 equipped with a diode-array detector. Mobile phases were gradients of 80% CH_3CN/20% H_2O (v/v) in 45 mM NH_4O_2CH at pH 3.5 and 0.5 ml/min. Purity was determined by monitoring at 330 ± 50 nm and was >95%. Final product purity was also assessed by combustion analysis carried out in the Campbell Microanalytical Laboratory, University of Otago, Dunedin, New Zealand. Melting points were determined on an Electrothermal 2300 Melting Point Apparatus. NMR spectra were obtained on a Bruker Avance 400 spectrometer at 400 MHz for ^{1}H and 100 MHz for ^{13}C spectra.

7.2. General procedures

A: Sulfonyl chloride (1 eq.) was dissolved in a mixture of dry DCM (0.2 M) and TEA (1.5 eq.). Amine (1.2 eq.) was added and the reaction was stirred at 20 °C until completion (TLC). The solvent was removed under reduced pressure and the crude product was purified by column flash-chromatography on silica to give the sulfonamide.

B: Aryl halide (1 eq.), CuI (1 eq.), *N*,*N*′-dimethylethylenediamine (2 eq.), amide (12 eq.) and K_2CO_3 (3 eq.) were dissolved in dry dioxane (0.2 M) and heated at 100 °C for 18–24 h. The mixture was cooled to 20 °C and solvent was removed under reduced pressure. The crude product was purified as for procedure A to give the amide [15].

C: $Pd(OAc)_2$, (0.01 eq.), Xantphos (0.015 eq.), amide (1.2 eq.), aryl halogen (1.0 eq.) and 1,4 dioxane (1 M) were heated at 100 °C for 24 h. The mixture was cooled to 20 °C, filtered, the solvent evaporated under reduced pressure and the crude product was purified as for procedure A to give the amide [16].

D: The aryl amine was dissolved in DMSO (0.8 M) and anhydride/acid chloride added to the solution and the mixture was heated for 12–18 h at 120 °C. The reaction was allowed to cool to 20 °C, diluted with EtOAc and washed with water, and the crude product was purified as for procedure A to give the amide [17].

E: The compound was dissolved in EtOAc (0.2 M) and 10% Pd/C (10 wt%) was added. The resulting mixture was stirred under H_2 (5 atm) for 8 h at 20 °C. The mixture was filtered through celite, the solvent evaporated and the crude was purified for procedure A to give the amine.

Table 4
IC_{50} values for compounds **9**, **12**, **14**, **15**, **17** against recombinant AKR1C3 and in HCT-116/AKR1C3 cells.

No	IC_{50} (nM)	
	AKR1C3[a]	HCT-116[b]
4	13	27
9	52	24
12	94	11
14	88	19
15	84	15
17	56	22

[a] As for Table 2.
[b] Concentration of drug to inhibit the conversion of nitroaromatic prodrug PR-104A to the hydroxylamine PR-104H in HCT-116 cells engineered to over-express AKR1C3, as determined by LC/MS/MS; see Experimental section.

7.3. Compounds of Table 2

7.3.1. 1-(4-(Piperidin-1-ylsulfonyl)phenyl)pyrrolidin-2-one (*10*) by procedures A and B (Scheme 1A)

4-Bromobenzenesulfonyl chloride (**36a**) (1 g, 3.90 mmol, 1 eq.) was dissolved in a mixture of dry DCM (50 ml, 0.2 M) and TEA (591 μl, 5.85 mmol, 1.5 eq.). piperidine (**52a**) (460 μl, 4.68 mmol, 1.2 eq.) was added and the reaction was stirred at 20 °C until completion (TLC). The solvent was removed under reduced pressure and the crude product was purified by column flash-chromatography on silica to give 1-(4-bromophenylsulfonyl) piperidine (**38a**) (1.19 g, 3.9 mmol, quantitative yield). ^{1}H NMR ($CDCl_3$) δ 7.67 (dt, J = 8.72, 2.16 Hz, 2H), 7.61 (dt, J = 8.72, 2.16 Hz, 2H), 2.99 (t, J = 5.48 Hz, 4H), 1.89 (m_c, 4H), 1.44 (m_c, 2H). This was used directly.

A mixture of **38a** (92 mg, 303 μmol, 1 eq.), CuI (58 mg, 303 μmol, 1 eq.), *N*,*N*′-dimethylethylenediamine (606 μmol, 2 eq.), pyrrolidin-2-one (350 mg, 3.63 mmol, 12 eq.) and K_2CO_3 (90 mg, 606 μmol, 3 eq.) were dissolved in dry dioxane (5 ml, 0.2 M) and heated at 100 °C for 18–24 h. The mixture was cooled to 20 °C and solvent was removed under reduced pressure. The crude product was purified as for procedure A to give **10** (48% yield). mp 180–182 °C. ^{1}H NMR ($CDCl_3$) δ 7.81 (td, J = 9.05, 2.28 Hz, 2H), 7.75 (td, J = 9.08, 2.16 Hz, 2H), 3.91 (t, J = 7.00 Hz, 2H), 2.98 (t, J = 5.44 Hz, 4H), 2.66 (t, J = 7.92 Hz, 2H), 2.21 (m_c, 2H), 1.64 (m_c, 4H), 1.41 (m_c, 2H). HRMS (ESI): $m/z = [M + H]^+$ calculated for $C_{15}H_{21}N_2O_3S$: 309.1267; found: 309.1276; $[M + Na]^+$ calculated for $C_{15}H_{20}N_2O_3SNa$: 331.1087; found: 331.1093; HPLC purity: 99.6%. Anal calcd for $C_{15}H_{20}N_2O_3S$: C, 58.42; H, 6.54: N, 9.08. Found: C, 58.40; H, 6.54: N, 8.85.

See Supplementary Material for details of the syntheses of related compounds **11**–**23** from **36a** and substituted piperidines **37b**–**k**.

7.4. Compounds of Table 3

7.4.1. 1-(4-(2-Methylpiperidin-1-ylsulfonyl)phenyl)azetidin-2-one (*24*)

Coupling of 1-(4-iodophenylsulfonyl)-2-methylpiperidine (**36b**) and azetidin-2-one by procedure B gave **24** (yield 92%); mp 149–

151 °C. ^{1}H NMR ($CDCl_3$) δ 7.79 (m_c, 4H), 4.23 (m_c, 1H), 3.90 (t, J = 7.08 Hz, 2H), 3.70 (td, J = 15.40, 1.60 Hz, 1H), 2.98 (dt, J = 12.80, 2.48 Hz, 1H), 2.65 (t, J = 7.93 Hz, 2H), 2.20 (m_c, 2 H), 1.65–1.33 (m, 5H), 1.08 (d, J = 6.88 Hz, 3H). HRMS (ESI): $m/z = [M + H]^+$ calculated for $C_{15}H_{21}N_2O_3S$: 309.1267; found: 309.1268; $[M + Na]^+$ calculated for $C_{15}H_{20}N_2O_3SNa$: 331.1087; found: 331.1082; HPLC purity: 99.8%. Anal calcd for $C_{15}H_{20}N_2O_3S \cdot 0.25H_2O$: C, 57.58; H, 6.60; N, 8.95. Found: C, 57.70; H, 6.27; N, 8.70.

7.4.2. 1-(4-(2-Methylpiperidin-1-ylsulfonyl)phenyl)piperidin-2-one (**25**)

Coupling of **36b** and piperidinone by procedure C gave **25** (4% yield); mp 124–126 °C. ^{1}H NMR ($CDCl_3$) δ 7.82 (td, J = 8.77, 2.48 Hz, 2H), 742 (td, J = 8.85, 2.44 Hz, 2H), 4.25 (m_c, 1H), 3.74–3.62 (m, 3H), 3.00 (dt, J = 12.68, 2.48 Hz, 1H), 2.58 (t, J = 6.52 Hz, 2H), 2.20–1.90 (m_c, 4H), 1.70–1.32 (m, 5H), 1.11 (d, J = 6.89 Hz, 3H). HRMS (ESI): $m/z = [M + H]^+$ calculated for $C_{17}H_{25}N_2O_3S$: 337.1580; found: 337.1576; $[M + Na]^+$ calculated for $C_{17}H_{24}N_2O_3SNa$: 359.1400; found: 359.1393. HPLC purity: 99.3%.

7.4.3. 1-(3-(2-Methylpiperidin-1-ylsulfonyl)phenyl)pyrrolidin-2-one (**26**)

Reaction of 3-bromobenzenesulfonyl chloride (**36l**) and 2-methylpiperidine by procedure A gave 1-(3-bromophenylsulfonyl)-2-methylpiperidine (**38l**) (93% yield). ^{1}H NMR ($CDCl_3$) δ 7.97 (t, J = 1.76 Hz, 1H), 7.75 (d, J = 7.80 Hz, 1H), 7.66 (td, J = 8.01, 0.80 Hz, 1H), 7.36 (t, J = 7.92 Hz, 1H), 4.24 (m_c, 1H), 3.72 (td, J = 13.49, 2.72 Hz, 1H), 3.01 (dt, J = 12.93, 2.52 Hz, 1H), 1.67–1.23 (m, 5H), 1.09 (d, J = 6.92 Hz, 3H). This was used directly.

Coupling of **38l** and 2-pyrrolidone by procedure B gave **26** (61% yield); mp 116–118 °C. ^{1}H NMR ($CDCl_3$) δ = 7.99–7.95 (m, 1H), 7.94 (dd, J = 2.24, 1.00 Hz, 1H), 7.59 (ddd, J = 7.76, 1.52, 1.08 Hz, 1H), 7.49 (dd, J = 15.89, 7.73 Hz, 1H), 4.25 (m_c, 1H), 3.90 (t, J = 7.04 Hz, 2H), 3.73 (td, J = 13.33, 3.80 Hz, 1H), 3.02 (dt, J = 12.65, 2.56 Hz, 1H), 2.63 (t, J = 7.89 Hz, 2H), 2.20 (m_c, 2H), 1.70–133 (m, 5H), 1.10 (d, J = 6.92 Hz, 3H) HRMS (ESI): $m/z = [M + H]^+$ calculated for $C_{17}H_{23}N_2O_3S$: 323.1424; found: 323.1426; $[M + Na]^+$ calculated for $C_{17}H_{21}N_2O_3SNa$: 345.1243; found: 345.1238; HPLC purity: 100%. Anal calcd for $C_{16}H_{22}N_2O_3S$: C, 59.60; H, 6.88; N, 8.69. Found: C, 59.60; H, 6.76; N, 8.65.

See Supplementary Information for details of the syntheses of related compounds **27**–**30** from benzenesulfonyl chlorides **36a**,**b**, **l**–**p**.

7.4.4. 1-(4-(2-Methylpiperidin-1-ylsulfonyl)phenyl)pyrrolidine-2,5-dione (**31**)

Reaction of 4-nitrobenzenesulfonyl chloride and 2-methyl piperidine by procedure A gave 2-methyl-1-(4-nitrophenylsulfonyl) piperidine (**38q**) (91% yield). ^{1}H NMR ($CDCl_3$) δ 8.34 (td, J = 8.93, 2.36 Hz, 2H), 8.00 (td, J = 8.96, 2.32 Hz, 2H), 4.334.23 (m, 1H), 3.76 (ddd, J = 13.12, 5.40, 2.16 Hz, 1H), 3.04 (dt, J = 12.88, 2.40 Hz, 1H), 1.67–1.30 (m, 5H), 1.11 (d, J = 6.92 Hz, 3H). HRMS (ESI): $m/z = [M + H]^+$ calculated for $C_{12}H_{17}N_2O_4S$: 285.0904; found: 285.0903; $[M + Na]^+$ calculated for $C_{12}H_{16}N_2O_4SNa$: 307.0723; found: 307.0720, HPLC purity: 99.7%.

Hydrogenation of **38q** by procedure E gave 4-(2-methylpiperidin-1-ylsulfonyl)aniline (**38r**) (97% yield). ^{1}H NMR ($CDCl_3$) δ 7.59 (d, J = 8.60 Hz, 2H), 6.66 (td, J = 8.69, 2.68 Hz, 2H), 4.19 (m_c, 1H), 4.05 (s_{br}, 2H), 3.64 (td, J = 13.21, 3.48 Hz, 1H), 2.95 (dt, J = 12.61, 2.32 Hz, 1H), 1.70–1.30 (m, 5H), 1.08 (d, J = 6.88 Hz, 3H). HRMS (ESI): $m/z = [M + H]^+$ calculated for $C_{12}H_{19}N_2O_2S$: 255.1162; found: 255.1157; $[M + Na]^+$ calculated for $C_{12}H_{18}N_2O_2SNa$: 277.0981; found: 277.0973. HPLC purity: 99.9%.

Coupling of **38r** with succinic anhydride by procedure D gave **31** (yield 44%); mp 203–206 °C. ^{1}H NMR ($CDCl_3$) δ = 7.92 (td, J = 8.80, 2.32 Hz, 2H), 7.50 (td, J = 8.85, 2.28 Hz, 2H), 4.31–4.21 (m, 1H), 3.71 (td, J = 13.36, 3.81 Hz, 1H), 3.01 (dt, J = 12.81, 2.52 Hz, 1H), 2.92 (s_{br}, 4H), 1.68–1.32 (m, 5H), 1.11 (d, J = 6.93 Hz, 3\H). HRMS (ESI): $m/z = [M + H]^+$ calculated for $C_{16}H_{21}N_2O_4S$: 337.1217; found: 337.1208; $[M + Na]^+$ calculated for $C_{16}H_{20}N_2O_4SNa$: 359.1036; found: 359.1029. HPLC purity: 99.1%. Anal calcd for $C_{16}H_{20}N_2O_4S$: C, 57.12; H, 5.99; N, 8.33. Found: C, 55.60; H, 6.02; N, 7.88.

See Supplementary Material for details of the syntheses of related compounds **32**–**35** from benzenesulfonamide **38r**.

7.5. COX assays

COX assays were carried out by GVK Biosciences Ltd., Biology, 28A, IDA Nacharam, Hyderabad 500 076 India: www.gvkbio.com

7.6. Production and purification of recombinant AKR1C protein

Recombinant AKR1C3 protein was purified from a plasmid vector incorporating the amplified gene in *Escherichia coli* BL21 (DE3) cells as described elsewhere [4]. AKR1C1, AKR1C2 and AKR1C4 protein was purified in the same method from expression vectors supplied as a gift by Dr Chris Bunce, University of Birmingham.

7.7. Inhibition of AKR1C enzyme activity

The AKR1C enzyme inhibitory activity of the compounds was determined by measuring their ability to prevent AKR1C-dependent reduction of a non-fluorescent ketone probe, Probe 5, to a fluorescent alcohol in the presence of NADPH as previously described [4]. The compounds and known AKR1C3 inhibitors (flufenamic acid, meclofenamic acid and mefenamic acid; Sigma–Aldrich, Auckland, New Zealand) were tested at multiple concentrations in duplicate between 0.1 nM and 100 μM in 2% DMSO to generate AKR1C enzyme inhibition data. Compound IC_{50} values were calculated by fitting the inhibition data to a four-parameter logistic sigmoidal dose–response curve using Prism 5.02 (GraphPad, La Jolla, CA, USA). All IC_{50} values <10 μM are reported as the mean of 2 or more separate determinations.

7.8. Inhibition of cellular AKR1C3 activity

The cellular AKR1C3 inhibitory activity of the compounds was determined in HCT-116 cells engineered to over-express AKR1C3 by measuring the inhibition of AKR1C3-dependent aerobic metabolism of an exogenous substrate (PR-104A) to its hydroxylamine metabolite (PR-104H). The quantitation of PR-104H by LC-MS/MS and transfection of the HCT-116/AKR1C3 cell line have been described previously [3,13]. Compound IC_{50} values were calculated from four-parameter logistic sigmoidal dose–response curves that were fitted to the inhibition data using Prism 5.02. See Supplementary Material for the structures of PR-10A and PR-104H.

Acknowledgements

This work was partially funded by the Deutsche Forschungsgemeinschaft under grant HE6009/1–1. (to D.H.). We thank Ms Emma Hamilton for help with the enzyme studies, Dr Chris Guise and Dr Adam Patterson for the HCT-116/AKR1C3 cell line, and Dr Chris Bunce for the AKR1C1, AKR1C2 and AKR1C4 expression vectors, and the New Zealand National eScience Infrastructure for access to computational support.

Appendix A. Supplementary data

Supplementary data related to this article can be found at http://dx.doi.org/10.1016/j.ejmech.2013.01.047.

References

[1] M.C. Byrns, Y. Jin, T.M. Penning, J. Steroid. Biochem. Mol. Biol. 125 (2011) 95–104.
[2] J.C. Desmond, J.C. Mountford, M.T. Drayson, E.A. Walker, M. Hewison, J.P. Ride, Q.T. Luong, R.E. Hayden, E.F. Vanin, C.M. Bunce, Cancer Res. 63 (2003) 505–512.
[3] T.M. Penning, M.E. Burczynski, L.M. Jez, H.-K. Lin, H. Ma, M. Moore, K. Ratnam, N. Palackal, Mol. Cell. Endocrinol. 171 (2001) 137–149.
[4] S.M.F. Jamieson, D.G. Brooke, D. Heinrich, G.J. Atwell, S. Silva, E.J. Hamilton, A.P. Turnbull, L.J.M. Rigoreau, E. Trivier, C. Soudy, S.S. Samlal, P.J. Owen, E. Schroeder, T. Raynham, J.U. Flanagan, W.A. Denny, J. Med. Chem. 55 (2012) 7746–7758.
[5] A.O. Adeniji, B.M. Twenter, M.C. Byrns, Y. Jin, M. Chen, J.D. Winkler, T.M. Penning, J. Med. Chem. 55 (2012) 2311–2323.
[6] J.M. Jez, M.J. Bennett, B.P. Schlegel, M. Lewis, T.M. Penning, Biochem. J. 326 (1997) 625–636.
[7] A.L. Lovering, J.P. Ride, C.M. Bunce, J.C. Desmond, S.M. Cummings, S.A. White, Cancer Res. 64 (2004) 1802–1810.
[8] M.C. Byrns, T.M. Penning, Chem. Biol. Interact. 178 (2009) 221–227.
[9] D.R. Bauman, S.L. Rudnick, L.M. Szewczuk, Y. Jin, S. Gopishetty, T.M. Penning, Mol. Pharmacol. 67 (2005) 60–68.
[10] V.J. Jackson, Y. Yosaamadja, J.U. Flanagan, C.J. Squire, Acta Crystallogr. F68 (2012) 409–413.
[11] J.U. Flanagan, Y. Yossatmadja, R.M. Teague, M.Z.L. Chai, A.P. Turnbull, C.J. Squire, PLoS One 7 (8) e43965, doi:10.1371/journal.pone.0043965.
[12] T. Ogihara, I. Tamai, A. Tsuji, A. J. Pharm. Sci. 88 (1999) 1217–1221.
[13] D.J. Yee, V. Balsanek, D. Sames, J. Am. Chem. Soc. 126 (2004) 2282–2283.
[14] C.P. Guise, M.R. Abbattista, R.S. Singleton, S.D. Holford, J. Connolly, G.U. Dachs, S.B. Fox, R. Pollock, J. Harvey, P. Guilford, F. Donate, W.R. Wilson, A.V. Patterson, Cancer Res. 70 (2010) 1573–1584.
[15] A. Klapars, X. Huang, S.L. Buchwald, A general and efficient copper catalyst for the amidation of aryl halides, J. Am. Chem. Soc. 124 (2004) 7421–7428.
[16] J. Yin, S.L. Buchwald, Org. Lett. 2 (2000) 1101–1104.
[17] J.J. Cui. WO 2004/76412 A2, published 10th Sept 2004.
[18] T.D. Warner, F. Giuliano, L. Vojnovic, A. Bukasa, J.A. Mitchell, J.R. Vane, Proc. Natl. Acad. Sci. U. S. A. 96 (1999) 7563–7568.